Acta Cryst E CRYSTALLOGRAPHIC COMMUNICATIONS

ISSN 2056-9890

Crystal structure and Hirshfeld surface analysis of 2,4,6-triaminopyrimidine-1,3-diium dinitrate

Sumra Dilshad,[a] Emine Berrin Çınar,[b] Arif Ali,[a] Adeeba Ahmed,[a] Mohd Jane Alam,[c] Musheer Ahmad,[a] Aiman Ahmad,[a] Necmi Dege[b] and Eiad Saif[d]*

[a]Department of Applied Chemistry, Faculty of Engineering and Technology, ZHCET, Aligarh Muslim University, Aligarh (UP), India, [b]Department of Physics, Faculty of Arts and Sciences, Ondokuz Mayıs University, Samsun, 55200, Turkey, [c]Department of Physics, Faculty of Science, Aligarh Muslim University, Aligarh, (UP), India, and [d]Department of Computer and Electronic Engineering Technology, Sanaa Community, College, Sanaa, Yemen. *Correspondence e-mail: eiad.saif@scc.edu.ye

Received 16 February 2022
Accepted 19 May 2022

Edited by J. T. Mague, Tulane University, USA

Keywords: crystal structure; energy framework; Hirshfeld surface; hydrogen bond; pyrimidine.

CCDC reference: 2173730

Supporting information: this article has supporting information at journals.iucr.org/e

The title compound, $C_4H_9N_5^{2+}\cdot 2NO_3^-$, crystallizes in the monoclinic crystal system, space group $P2_1/c$. The asymmetric unit, which comprises a diprotonated triaminopyrimidine dication and two nitrate anions, has an almost planar geometry with a dihedral angle of 0.92 (4)° between the mean plane of the cation and that defined by both anions. In the crystal, hydrogen-bonding interactions between the 2,4,6-triaminopyrimidine cation and the nitrate anions lead to a one-dimensional supramolecular network with weak anionic interactions forming a three-dimensional network. These interactions were investigated using Hirshfeld surface analysis, which indicates that the most important contributions for the packing arrangement are from O···H/H···O (53.2%), N···H/H···N (12.5%) and C···H/H···C (9.6%) interactions. Energy framework analysis showed that of the components of the framework energies, electrostatic repulsion (E_{rep}) is dominant.

1. Chemical context

Nitrogen heterocycles and pyrimidines are examples of the most important biologically active compounds and find wide use in modern medicine (Pałasz & Cież, 2015; Takeshita *et al.*, 2006; Henderson *et al.*, 2003). Pyrimidine derivatives are used as intermediates for the production of various complex organic molecules for the treatment of cancer and AIDS (Fawcett *et al.*, 1996). Several pyrimidine derivatives belong to the class of central nervous system depressants (Soayed *et al.*, 2015). Pyrimidine and its derivatives have great importance as they constitute a significant class of natural and non-natural products, many of which possess remarkable biological activities and clinical applications such as antibacterial, antimalarial and anticancer agents (Sharma *et al.*, 2014). Many pyrimidine derivatives are reported to possess potential central nervous system (CNS) depressant properties and also act as calcium channel blockers (Kumar *et al.*, 2002). Pyrimido[4,5-*d*]pyrimidine-2,5-dione and 2,4-diamino-5-(substituted)pyrimidines have been reported to have potent antimicrobial activity (Sharma *et al.*, 2004) and 2,4,6-triaminopyrimidine (TAP) acts as a fast-killing and long-acting antimalarial agent (Hameed, *et al.*, 2015). It is also known to inhibit sodium transport in the skin of frogs (Bowman *et al.*, 1978). It can be synthesized by a regioselective cycloaddition process in high yield by reaction between two moles of

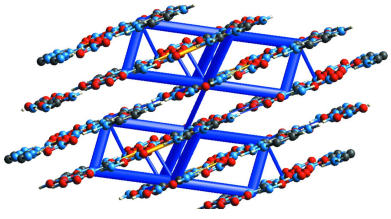

cyanamide and one mole of ynamide in the presence of triflic acid as catalyst (Dubovtsev, *et al.*, 2021). Many pyrimidine derivatives display interesting optical and sensing properties (Achelle *et al.*, 2012, Seenan *et al.*, 2020). Methylpyrimidinium push–pull derivatives have been shown to be promising materials for optical data processing. Organometallic methylpyrimidinium chromophores incorporating a ruthenium fragment within the π-conjugated spacer are among the best metal–diyne NLO chromophores (Fecková, *et al.*, 2020). Herein, we report the structure of 2,4,6-triamino-1,3,5-triazine-1,3-diium dinitrate, Fig. 1, which was synthesized *via* reaction of 2,4,6-triaminopyrimidine with nitric acid.

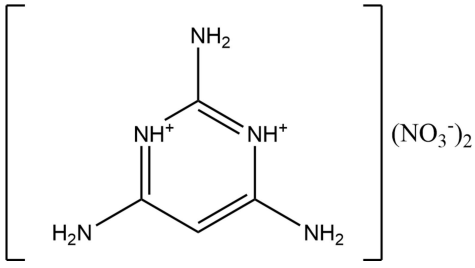

2. Structural commentary

In the asymmetric unit, the mean planes of the nitrate anions are inclined to one another by 5.97 (8)°. The plane of the anion containing N6 is inclined to the mean plane of the cation by 3.25 (6)° while that of the other anion is inclined by 2.84 (6)°. Thus the whole asymmetric unit lies close to a common plane (Fig.1). The ring C—N bond lengths in the cation [C1—N2 = 1.3531 (16) Å and C2—N3 = 1.3267 (16) Å] are only slightly altered from those in the corresponding conjugate base (Schwalbe *et al.*, 1982). The C—C bond lengths in the pyrimidine ring [C2—C3 = 1.3834 (18) and C3—C4 = 1.3888 (17) Å] are consistent with literature values (Ali *et al.*, 2021). The exocyclic C2—N3 and C4—N4 bond lengths [1.3267 (16) and 1.3240 (17) Å, respectively] are equivalent within experimental error but the C1—N1 bond length is markedly shorter at 1.3010 (17) Å. As it lies between the two protonated ring nitrogen atoms, this suggests that the neighboring positive charge induces a contribution from a charge-separated quinoid form to the overall electronic structure, as has been proposed for the analogous chloride salt (Portalone & Colapietro, 2007)

Table 1
Hydrogen-bond geometry (Å, °).

D—H···A	D—H	H···A	D···A	D—H···A
N5—H5···O4	0.86	1.88	2.7321 (15)	174
N2—H2···O1^{i}	0.86	1.98	2.8319 (15)	169
N4—H4*A*···O6	0.86	2.08	2.9428 (15)	177
N4—H4*B*···O5^{ii}	0.86	2.43	3.0706 (16)	131
N4—H4*B*···O6^{ii}	0.86	2.11	2.9593 (15)	172
N1—H1*A*···O2	0.86	1.97	2.7986 (15)	160
N1—H1*B*···O3^{i}	0.86	1.94	2.7912 (15)	172
N3—H3*A*···O3^{iii}	0.86	2.16	3.0018 (14)	167
N3—H3*A*···O2^{iii}	0.86	2.54	2.9770 (15)	113
N3—H3*B*···O5^{iii}	0.86	2.26	3.0619 (15)	156
C3—H3···O5^{iii}	0.93	2.56	3.3134 (16)	139

Symmetry codes: (i) $-x+1, y-\frac{1}{2}, -z+\frac{3}{2}$; (ii) $-x+2, y-\frac{1}{2}, -z+\frac{1}{2}$; (iii) $x, y-1, z$.

3. Supramolecular features

In the crystal, a combination of N1—H1*A*···O2, N5—H5···O4, N4—H4*A*···O6, N3—H1*A*···O3 and N3—H3*B*···O5 hydrogen bonds (Table 1) leads to the formation of ribbons of alternating cations and anions extending along the *b*-axis direction. The mean planes of the ribbons are parallel to (101). Pairs of adjacent ribbons are linked by N1—H1*B*···O3, N2—H2···O1 and N3—H3*A*···O3 hydrogen bonds (Table 1), with these units further connected into cation/anion layers by complementary N4—H4*B*···O6 hydrogen bonds. The two unique nitrate ions are connected to the cation by N—H···O hydrogen bonds (Table 1), forming units with an $R_2^2(8)$ graph-set motif (Fig. 2). This tight hydrogen-bonded network causes a short O2···O4 contact of 2.7752 (15) Å. Finally, the layers appear to be associated through N═O···π(ring) interactions N6═O3···*Cg*1^{i} and N7═O5···*Cg*1^{ii} (*Cg*1^{i} is the centroid of the pyrimidine ring at $-x+1, -y+1, -z+1$; *Cg*^{ii} is the

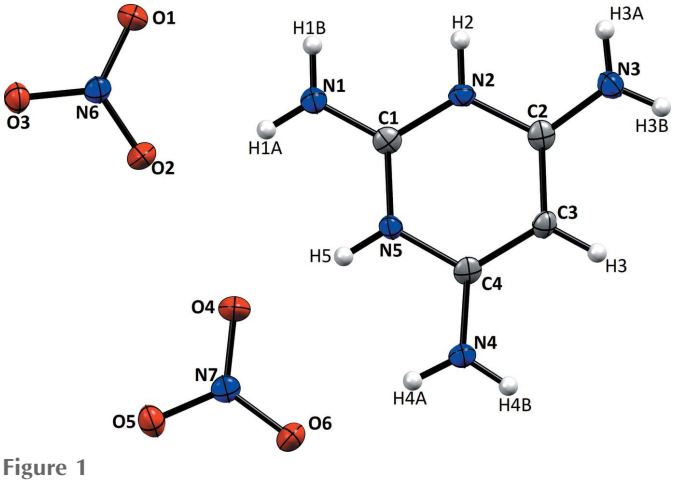

Figure 1
ORTEP diagram of the title compound with atom labeling and 50% probability ellipsoids.

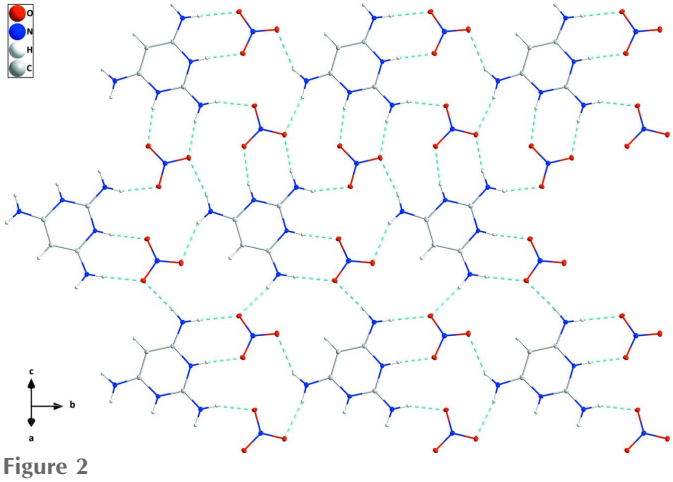

Figure 2
A portion of one cation/anion layer projected onto (101) with N—H···O hydrogen bonds depicted by dashed lines.

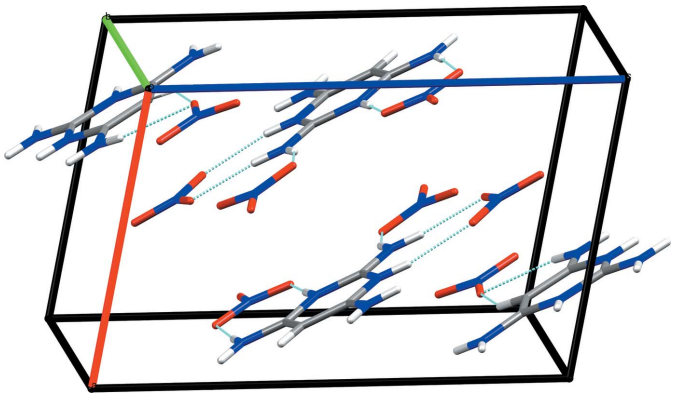

Figure 3
Packing view of the title compound showing the anionic–π interaction that forms the supramolecular structure.

centroid of the pyrimidine ring at $-x+2, -y+1, -z+1$) with O3···*Cg*1^{i} = 3.1369 (11) Å, N6···*Cg*1^{i} = 3.4241 (12) Å, N6═O3···*Cg*1^{i} = 92.16 (7)°; O5···*Cg*1^{ii} = 3.0265 (11) Å; N7···*Cg*1^{ii} = 3.5176 (12) Å; N7═O5···*Cg*1^{ii} = 102.62 (7)° (Fig. 3).

4. Hirshfeld Surface Analysis

The Hirshfeld surface analysis (Spackman & Jayatilaka *et al.* 2009) was performed and the two-dimensional fingerprint plots (McKinnon *et al.*, 2007) were generated with *Crystal Explorer17* (Turner *et al.*, 2017) to quantify the intermolecular contacts present within the crystal structure.

The Hirshfeld surface is mapped over d_{norm} in the range −0.6823 to 0.9826 in arbitrary units with colors ranging from red (shorter distance than the sum of van der Waals radii) through white to blue (longer distance than the sum of the van der Waals radii). Top and bottom views of the surface together with curvedness, and shape-index plots are given in Fig. 4*a*–*d*. The red spots symbolize N—H···O contacts and C—H···O interactions. The fingerprint plots (Fig. 5) give an insight into the overall packing characteristics of the contents of the unit cell, being plots of d_e *versus* d_i, where d_i is the distance to the nearest atom center interior to the surface, and d_e to the nearest atom exterior to the surface. These plots show that the main contributions to the overall surface involve O···H/H···O contacts at 53.2% (Fig. 5*b*), followed by N···H/H···N contacts at 12.5% (Fig. 5*c*) and C···H/H···C contacts at 9.6% (Fig. 5*d*).

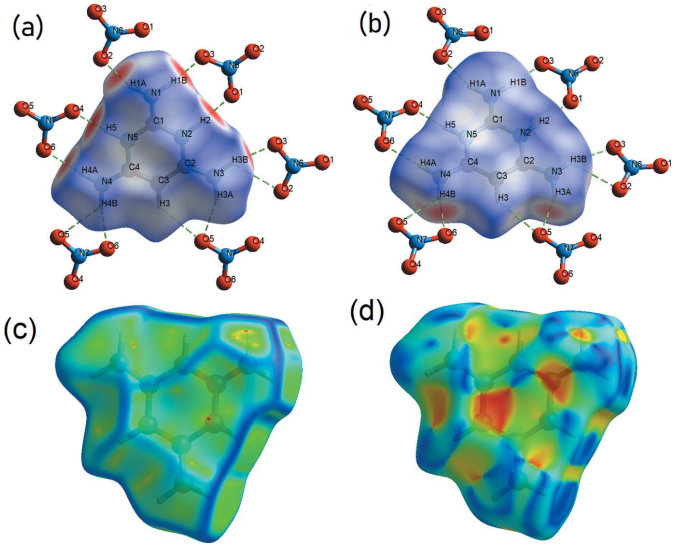

Figure 4
The Hirshfeld surface of the title complex mapped over (*a*) d_{norm} (top view), (*b*) d_{norm} (bottom view), (*c*) curvedness and (*d*) shape-index.

5. Synthesis and crystallization

To synthesize the title compound, 20 mg of 2,4,6-triaminopyrimidine were dissolved in ethanol (10 mL) and the solution stirred for 3 h. A mixture of ethanol (5 mL) and nitric acid (0.5 mL) was taken in a separate round-bottom flask and stirred for 3 h at 333 K. Afterwards, the 2,4,6-triamino-

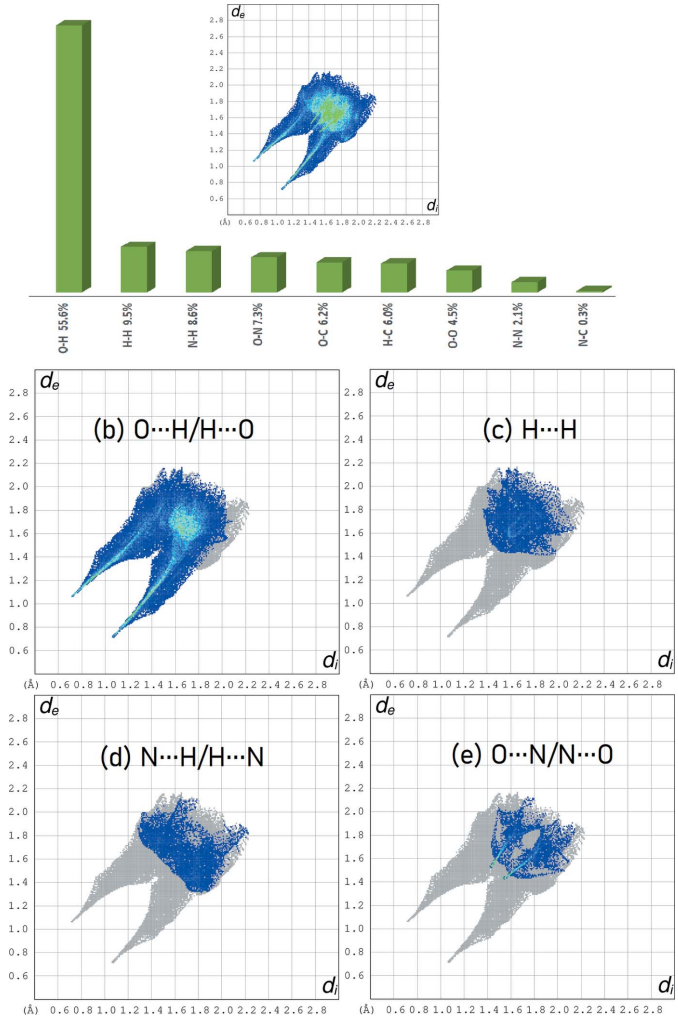

Figure 5
(*a*) The overall two-dimensional fingerprint plot, and those delineated into (*b*) O···H/H···O, (*c*) N···H/H···N and (*d*) C···H/H···C interactions.

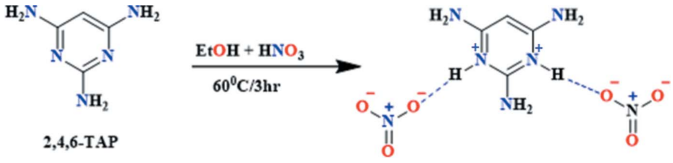

Figure 6
Synthesis of title compound.

pyrimidine solution was added dropwise to the above mixture. The reaction was continued for 4 h at the same temperature. After completion of the reaction, a pale-yellow solution was obtained, which was filtered and kept for slow evaporation at room temperature. After 15 days, pale-yellow crystals were obtained that were suitable for data collection (Fig. 6).

6. Interaction energy calculations

The interaction energies for the title compound (Fig. 7). were computed using the HF/3-21G quantum level of theory, which is available in *CrystalExplorer 17.5*. Electrostatic (E_{ele}), polarization (E_{pol}), dispersion (E_{disp}), and exchange-repulsion (E_{rep}) are the four energy variables that make up the total intermolecular interaction energy (E_{tot}). Cylinder-shaped energy frameworks represent the relative strengths of interaction energies in individual directions and give the topologies of pair-wise intermolecular interaction energies within the crystal (Mackenzie *et al.*, 2017). The energies between molecular pairs are represented as cylinders connecting the centroids of pairs of molecules, with the cylinder radius equal to the amount of interaction energy between the molecules (Wu *et al.*, 2020). The dark-blue-colored molecule at symmetry position (x, $-y+\frac{1}{2}$, $z+\frac{1}{2}$) located 6.25 Å from the centroid of the selected molecule has the highest total interaction energy of -40.1 kJ mol^{-1}, as shown in Fig.7. The net interaction energies for the title compound are $E_{ele} = -58.9$ kJ mol^{-1}, $E_{pol} = -92.0$ kJ mol^{-1}, $E_{dis} = -148.8$ kJ mol^{-1}, $E_{rep} = 176.9$ kJ mol^{-1}, with a total interaction energy E_{tot} of -110.4 kJ mol^{-1} (Fig. 8). Clearly, E_{rep} is the major interaction energy in the title compound.

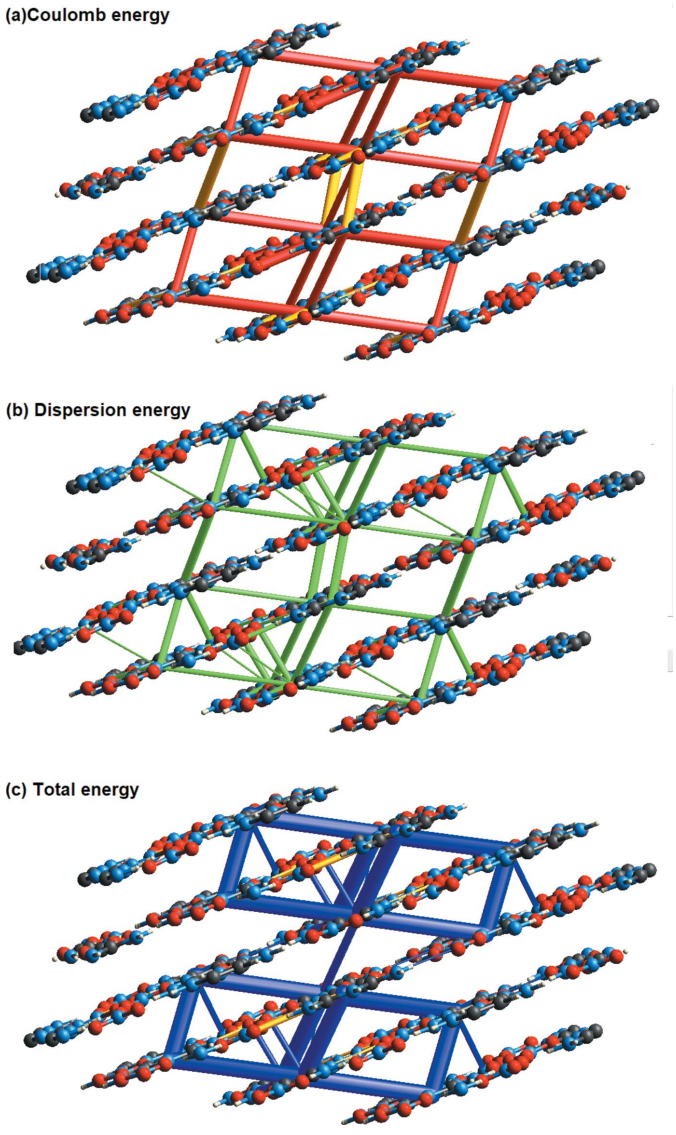

Figure 8
Energy frameworks for a 2×2×2 supercell viewed down the crystallographic *b* axis for the threefold interpenetrated crystal structure. The red-colored frame shows the Coulombic energy, green shows dispersion, and blue shows total energy.

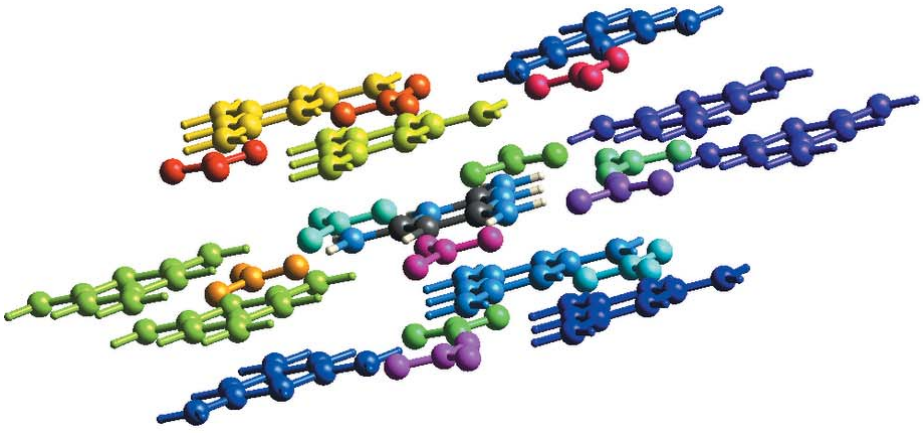

	N	Symop	R	Electron Density	E_ele	E_pol	E_dis	E_rep	E_tot
	1	-	6.32	HF/3-21G	1.6	-0.4	-2.9	0.5	-0.9
	1	-	3.50	HF/3-21G	0.0	nan	0.0	0.0	nan
	1	-	5.77	HF/3-21G	0.0	-7.4	0.0	0.0	-4.8
	1	-x, -y, -z	7.29	HF/3-21G	-15.4	-1.9	-3.4	0.0	-20.0
	1	-x, -y, -z	5.23	HF/3-21G	24.6	-16.9	-23.5	12.9	3.4
	2	-x, y+1/2, -z+1/2	9.09	HF/3-21G	2.5	-0.2	-1.5	0.0	1.1
	1	-	5.86	HF/3-21G	-12.3	-5.3	-8.2	33.1	3.4
	1	-	3.41	HF/3-21G	-3.2	-5.4	-17.5	10.6	-13.9
	1	-	4.95	HF/3-21G	-24.0	-9.3	-11.8	69.2	14.9
	1	-	4.89	HF/3-21G	-15.4	-1.9	-3.4	0.0	-20.0
	1	-	5.81	HF/3-21G	2.0	-0.6	-1.0	0.0	0.8
	1	-x, -y, -z	7.50	HF/3-21G	0.6	-3.0	-4.1	0.1	-5.0
	2	x, -y+1/2, z+1/2	6.25	HF/3-21G	-26.9	-7.4	-13.7	4.2	-41.1
	1	-x, -y, -z	5.52	HF/3-21G	-20.0	-12.0	-19.5	6.6	-40.4
	2	-x, y+1/2, -z+1/2	9.51	HF/3-21G	8.2	-0.9	-1.0	0.0	6.9
	1	-	5.91	HF/3-21G	-8.6	-0.7	-8.4	25.4	3.8
	1	-	5.15	HF/3-21G	2.8	-1.3	-5.4	1.4	-1.7
	1	-	5.72	HF/3-21G	24.6	-16.9	-23.5	12.9	3.4
	1	-	5.56	HF/3-21G	0.0	-0.5	0.0	0.0	-0.3

Figure 7
Interaction energies for the title compound were calculated with the HF/3–21 G model.

Table 2
Experimental details.

Crystal data	
Chemical formula	$C_4H_9N_5^{2+}\cdot 2NO_3^-$
M_r	251.18
Crystal system, space group	Monoclinic, $P2_1/c$
Temperature (K)	276
a, b, c (Å)	7.8650 (5), 9.9173 (6), 12.2291 (7)
β (°)	100.836 (2)
V (Å^3)	936.86 (10)
Z	4
Radiation type	Mo $K\alpha$
μ (mm^{-1})	0.16
Crystal size (mm)	0.37 × 0.27 × 0.14
Data collection	
Diffractometer	Bruker APEXII CCD
No. of measured, independent and observed [$I > 2\sigma(I)$] reflections	13469, 2312, 1993
R_{int}	0.070
$(\sin\theta/\lambda)_{max}$ (Å^{-1})	0.668
Refinement	
$R[F^2 > 2\sigma(F^2)]$, $wR(F^2)$, S	0.040, 0.110, 1.07
No. of reflections	2312
No. of parameters	154
H-atom treatment	H-atom parameters constrained
$\Delta\rho_{max}$, $\Delta\rho_{min}$ (e Å^{-3})	0.51, −0.30

Computer programs: *X-AREA* and *X-RED32* (Stoe & Cie, 2002), *SHELXT2018/3* (Sheldrick, 2015*a*), *SHELXL2018/3* (Sheldrick, 2015*b*), *OLEX2* (Dolomanov *et al.*, 2009), *Mercury* (Macrae *et al.*, 2020), *WinGX* (Farrugia, 2012), *PLATON* (Spek, 2020) and *publCIF* (Westrip, 2010).

7. Database survey

A search of the Cambridge Structural Database (CSD, Version 5.43, update of March 2022; Groom *et al.*, 2016) for the triaminopyrimidine dication gave 24 hits of which 16 were for the FPO_3^{2-} salt studied at a variety of temperatures (GESWAF–GESWAF15; Matulková *et al.*, 2017) but no structure containing nitrate anions was found. The remaining structures contain arenesulfonate (TEYTEZ, TEYTID and TEYXIH; Karak *et al.*, 2018), various polycarboxylate (VEXQEX, VEXZUW and VEYBEJ; Xing, *et al.*, 2017), chloride (GIMROK; Portalone & Colapietro, 2007) and $[Cu_2Cl_8]^{4-}$ (GOHDOY; Voronina *et al.*, 2012) anions. Most of the discussions of these structures are concerned more with their supramolecular structures than the detailed geometry of the cation but, as noted in Section 3, some details similar to those in the present work are seen in the structure of the chloride salt.

8. Refinement

Crystal data, data collection and structure refinement details are summarized in Table 2. All H atoms were originally found in difference maps. Thy were positioned geometrically (N—H = 0.86 Å, C—H = 0.93 Å) and refined as riding with U_{iso}(H) = 1.2U_{eq}(C,N).

Acknowledgements

The authors are grateful to the Department of Applied Chemistry, Aligarh Muslim University, for providing laboratory facilities. Author contributions are as follows. Conceptualization, SD and EBÇ; methodology, AimanA and ArifA; investigation, SD and AdeebaA; writing (original draft), SD, EBÇ and ND; writing (review and editing of the manuscript), AimanA and ArifA; visualization, MA and AJA; supervision, ES and ND.

References

Achelle, S., Barsella, A., Baudequin, C., Caro, B. & Robin-le Guen, F. (2012). *J. Org. Chem.* **77**, 4087–4096.
Ali, A., Muslim, M., Kamaal, S., Ahmed, A., Ahmad, M., Shahid, M., Khan, J. A., Dege, N., Javed, S. & Mashrai, A. (2021). *Acta Cryst.* E**77**, 755–758.
Bowman, R. H., Arnow, J. & Weiner, I. M. (1978). *J. Pharmacol. Exp. Ther.* **206**, 207–217.
Dolomanov, O. V., Bourhis, L. J., Gildea, R. J., Howard, J. A. K. & Puschmann, H. (2009). *J. Appl. Cryst.* **42**, 339–341.
Dubovtsev, A. Y., Zvereva, V. V., Shcherbakov, N. V., Dar'in, D. V., Novikov, A. S. & Kukushkin, V. Y. (2021). *Org. Biomol. Chem.* **19**, 4577–4584.
Farrugia, L. J. (2012). *J. Appl. Cryst.* **45**, 849–854.
Fawcett, J., Henderson, W., Kemmitt, R. D. W., Russell, D. R. & Upreti, A. (1996). *J. Chem. Soc. Dalton Trans.* pp. 1897–1903.
Fecková, M., le Poul, P., Bureš, B., Robin-le Guen, F. & Achelle, S. (2020). *Dyes Pigments*, **182**, 108659–108712.
Groom, C. R., Bruno, I. J., Lightfoot, M. P. & Ward, S. C. (2016). *Acta Cryst.* B**72**, 171–179.
Hameed, P. S., Solapure, S., Patil, V., Henrich, P. P., Magistrado, P. A., Bharath, S., Murugan, K., Viswanath, P., Puttur, J., Srivastava, A., Bellale, E., Panduga, V., Shanbag, G., Awasthy, D., Landge, S., Morayya, S., Koushik, K., Saralaya, R., Raichurkar, A., Rautela, N., Roy Choudhury, N., Ambady, A., Nandishaiah, R., Reddy, J., Prabhakar, K. R., Menasinakai, S., Rudrapatna, S., Chatterji, M., Jiménez-Díaz, M. B., Martínez, M. S., Sanz, L. M., Coburn-Flynn, O., Fidock, D. A., Lukens, A. K., Wirth, D. F., Bandodkar, B., Mukherjee, K., McLaughlin, R. E., Waterson, D., Rosenbrier-Ribeiro, L., Hickling, K., Balasubramanian, V., Warner, P., Hosagrahara, V., Dudley, A., Iyer, P. S., Narayanan, S., Kavanagh, S. & Sambandamurthy, V. K. (2015). *Nat. Commun.* **6**, 6715–6721.
Henderson, J. P., Byun, J., Takeshita, J. & Heinecke, J. W. (2003). *J. Biol. Chem.* **278**, 23522–23528.
Karak, S., Kumar, S., Pachfule, P. & Banerjee, R. (2018). *J. Am. Chem. Soc.* **140**, 5138–5145.
Kumar, B., Kaur, B., Kaur, J., Parmar, A., Anand, R. D. & Kumar, H. (2002). *Indian J. Chem. Sect. B*, **41**, 1526–1530.
Mackenzie, C. F., Spackman, P. R., Jayatilaka, D. & Spackman, M. A. (2017). *IUCrJ*, **4**, 575–587.
Macrae, C. F., Sovago, I., Cottrell, S. J., Galek, P. T. A., McCabe, P., Pidcock, E., Platings, M., Shields, G. P., Stevens, J. S., Towler, M. & Wood, P. A. (2020). *J. Appl. Cryst.* **53**, 226–235.
Matulková, I., Fábry, J., Němec, I., Císařová, I. & Vaněk, P. (2017). *Acta Cryst.* B**73**, 1114–1124.
McKinnon, J. J., Jayatilaka, D. & Spackman, M. A. (2007). *Chem. Commun.* pp. 3814–3816.
Pałasz, A. & Cież, D. (2015). *Eur. J. Med. Chem.* **97**, 582–611.
Portalone, G. & Colapietro, M. (2007). *Acta Cryst.* C**63**, o655–o658.
Schwalbe, C. H. & Williams, G. J. B. (1982). *Acta Cryst.* B**38**, 1840–1843.
Seenan, S. & Iyer, S. K. (2020). *J. Org. Chem.* **85**, 1871–1881.
Sharma, P., Rane, N. & Gurram, V. K. (2004). *Bioorg. Med. Chem. Lett.* **14**, 4185–4190.
Sharma, V., Chitranshi, N. & Agarwal, A. J. (2014). *J. Med. Chem.* Article ID 202784. https://doi.org/10.1155/2014/202784
Sheldrick, G. M. (2015*a*). *Acta Cryst.* A**71**, 3–8.
Sheldrick, G. M. (2015*b*). *Acta Cryst.* C**71**, 3–8.

Soayed, A. A., Refaat, H. M. & Sinha, L. (2015). *J. Saudi Chem. Soc.* **19**, 217–226.
Spackman, M. A. & Jayatilaka, D. (2009). *CrystEngComm*, **11**, 19–32.
Spek, A. L. (2020). *Acta Cryst.* E**76**, 1–11.
Stoe & Cie (2002). *X-AREA* and *X-RED32*. Stoe & Cie GmbH, Darmstadt, Germany.
Takeshita, J., Byun, J., Nhan, T. Q., Pritchard, D. K., Pennathur, S., Schwartz, S. M., Chait, A. & Heinecke, J. W. (2006). *J. Biol. Chem.* **281**, 3096–3104.
Turner, M. J., McKinnon, J. J., Wolff, S. K., Grimwood, D. J., Spackman, P. R., Jayatilaka, D. & Spackman, M. A. (2017). *CrystalExplorer17*. University of Western Australia. http://hirshfeldsurface.net
Voronina, J., Neckljudov, G. B., Salnikov, Yu., Fattakhov, S. & Shulaeva, M. (2012). CSD *Communication* (refcode GOHDOY). CCDC, Cambridge, England.
Westrip, S. P. (2010). *J. Appl. Cryst.* **43**, 920–925.
Wu, Q., Xiao, J.-C., Zhou, C., Sun, J.-R., Huang, M.-F., Xu, X., Li, T. & Tian, H. (2020). *Crystals*, **10**, 334–348.
Xing, P., Li, Q., Li, Y., Wang, K., Zhang, Q. & Wang, L. (2017). *J. Mol. Struct.* **1136**, 59–68.

supporting information

Acta Cryst. (2022). E**78**, 669-674 [https://doi.org/10.1107/S2056989022005333]

Crystal structure and Hirshfeld surface analysis of 2,4,6-triaminopyrimidine-1,3-diium dinitrate

Sumra Dilshad, Emine Berrin Çınar, Arif Ali, Adeeba Ahmed, Mohd Jane Alam, Musheer Ahmad, Aiman Ahmad, Necmi Dege and Eiad Saif

Computing details

Data collection: *X-AREA* (Stoe & Cie, 2002); cell refinement: *X-AREA* (Stoe & Cie, 2002); data reduction: *X-RED32* (Stoe & Cie, 2002); program(s) used to solve structure: *SHELXT2018/3* (Sheldrick, 2015a); program(s) used to refine structure: *SHELXL2018/3* (Sheldrick, 2015b); molecular graphics: *OLEX2* (Dolomanov *et al.*, 2009) and *Mercury* (Macrae *et al.*, 2020); software used to prepare material for publication: *WinGX* (Farrugia, 2012), *SHELXL2018/3* (Sheldrick, 2015b), *PLATON* (Spek, 2020) and *publCIF* (Westrip, 2010).

2,4,6-Triaminopyrimidine-1,3-diium dinitrate

Crystal data

$C_4H_9N_5^{2+}\cdot 2NO_3^-$
M_r = 251.18
Monoclinic, $P2_1/c$
a = 7.8650 (5) Å
b = 9.9173 (6) Å
c = 12.2291 (7) Å
β = 100.836 (2)°
V = 936.86 (10) Å^3
Z = 4
$F(000)$ = 520
D_x = 1.781 Mg m^{-3}
Mo $K\alpha$ radiation, λ = 0.71073 Å
Cell parameters from 8448 reflections
θ = 2.3–25.6°
μ = 0.16 mm^{-1}
T = 276 K
Needle, colourless
0.37 × 0.27 × 0.14 mm

Data collection

Bruker APEXII CCD diffractometer
φ and ω scans
13469 measured reflections
2312 independent reflections
1993 reflections with $I > 2\sigma(I)$
R_{int} = 0.070
θ_{max} = 28.3°, θ_{min} = 2.6°
h = −10→10
k = −13→13
l = −16→16

Refinement

Refinement on F^2
Least-squares matrix: full
$R[F^2 > 2\sigma(F^2)]$ = 0.040
$wR(F^2)$ = 0.110
S = 1.07
2312 reflections
154 parameters
0 restraints
Hydrogen site location: inferred from neighbouring sites
H-atom parameters constrained
$w = 1/[\sigma^2(F_o^2) + (0.0497P)^2 + 0.4576P]$ where $P = (F_o^2 + 2F_c^2)/3$
$(\Delta/\sigma)_{max} < 0.001$
$\Delta\rho_{max}$ = 0.51 e Å^{-3}
$\Delta\rho_{min}$ = −0.30 e Å^{-3}

Special details

Geometry. All esds (except the esd in the dihedral angle between two l.s. planes) are estimated using the full covariance matrix. The cell esds are taken into account individually in the estimation of esds in distances, angles and torsion angles; correlations between esds in cell parameters are only used when they are defined by crystal symmetry. An approximate (isotropic) treatment of cell esds is used for estimating esds involving l.s. planes.

Fractional atomic coordinates and isotropic or equivalent isotropic displacement parameters (Å²)

	x	*y*	*z*	U_{iso}*/U_{eq}
O3	0.54263 (12)	0.80420 (9)	0.71416 (8)	0.0141 (2)
O5	0.88490 (13)	0.76472 (9)	0.36706 (8)	0.0148 (2)
O1	0.50750 (13)	0.59279 (10)	0.75438 (8)	0.0168 (2)
O6	0.93192 (13)	0.56691 (10)	0.30278 (8)	0.0173 (2)
O4	0.80491 (14)	0.58662 (10)	0.44532 (8)	0.0207 (2)
O2	0.64974 (14)	0.64786 (10)	0.62512 (9)	0.0205 (2)
N5	0.77821 (13)	0.31443 (11)	0.47214 (9)	0.0099 (2)
H5	0.787384	0.398958	0.458644	0.012*
N2	0.68341 (13)	0.14353 (11)	0.57534 (9)	0.0105 (2)
H2	0.634287	0.118719	0.629218	0.013*
N4	0.92308 (15)	0.27225 (11)	0.32949 (9)	0.0128 (2)
H4A	0.929637	0.358122	0.321423	0.015*
H4B	0.967123	0.218902	0.286854	0.015*
N6	0.56691 (14)	0.68070 (11)	0.69851 (9)	0.0115 (2)
N7	0.87310 (14)	0.63926 (11)	0.37153 (9)	0.0116 (2)
N1	0.63901 (14)	0.36592 (11)	0.61695 (9)	0.0130 (2)
H1A	0.649848	0.450490	0.604304	0.016*
H1B	0.588658	0.340225	0.670025	0.016*
N3	0.71841 (14)	−0.08175 (11)	0.53700 (9)	0.0131 (2)
H3A	0.666228	−0.100504	0.590919	0.016*
H3B	0.754039	−0.145693	0.499473	0.016*
C1	0.69879 (15)	0.27685 (13)	0.55581 (10)	0.0103 (3)
C4	0.84517 (15)	0.22217 (13)	0.40753 (10)	0.0101 (3)
C3	0.82632 (16)	0.08538 (12)	0.42648 (10)	0.0103 (3)
H3	0.868341	0.021484	0.382632	0.012*
C2	0.74394 (15)	0.04582 (13)	0.51170 (10)	0.0106 (2)

Atomic displacement parameters (Å²)

	U^{11}	U^{22}	U^{33}	U^{12}	U^{13}	U^{23}
O3	0.0184 (5)	0.0101 (4)	0.0138 (5)	0.0018 (3)	0.0028 (4)	−0.0004 (3)
O5	0.0195 (5)	0.0105 (5)	0.0130 (5)	−0.0005 (4)	−0.0006 (4)	0.0002 (3)
O1	0.0244 (5)	0.0126 (5)	0.0153 (5)	−0.0007 (4)	0.0088 (4)	0.0021 (3)
O6	0.0254 (5)	0.0144 (5)	0.0140 (5)	0.0018 (4)	0.0088 (4)	−0.0018 (4)
O4	0.0344 (6)	0.0149 (5)	0.0166 (5)	−0.0011 (4)	0.0142 (4)	0.0018 (4)
O2	0.0328 (6)	0.0141 (5)	0.0189 (5)	0.0008 (4)	0.0163 (4)	−0.0014 (4)
N5	0.0140 (5)	0.0081 (5)	0.0071 (5)	−0.0002 (4)	0.0005 (4)	0.0004 (4)
N2	0.0133 (5)	0.0113 (5)	0.0068 (5)	−0.0011 (4)	0.0018 (4)	0.0008 (4)
N4	0.0187 (5)	0.0116 (5)	0.0087 (5)	0.0005 (4)	0.0041 (4)	0.0004 (4)

N6	0.0140 (5)	0.0119 (5)	0.0077 (5)	0.0004 (4)	−0.0001 (4)	−0.0004 (4)
N7	0.0126 (5)	0.0133 (5)	0.0078 (5)	0.0003 (4)	−0.0014 (4)	0.0004 (4)
N1	0.0181 (5)	0.0106 (5)	0.0106 (5)	−0.0001 (4)	0.0033 (4)	0.0000 (4)
N3	0.0174 (5)	0.0101 (5)	0.0115 (5)	−0.0005 (4)	0.0020 (4)	0.0011 (4)
C1	0.0095 (5)	0.0127 (6)	0.0071 (5)	−0.0003 (4)	−0.0026 (4)	0.0002 (4)
C4	0.0103 (5)	0.0125 (6)	0.0056 (5)	0.0000 (4)	−0.0032 (4)	−0.0006 (4)
C3	0.0122 (5)	0.0107 (6)	0.0072 (5)	0.0009 (4)	−0.0006 (4)	−0.0015 (4)
C2	0.0095 (5)	0.0118 (6)	0.0082 (5)	0.0000 (4)	−0.0040 (4)	−0.0008 (4)

Geometric parameters (Å, º)

O3—N6	1.2597 (14)	N4—C4	1.3240 (17)
O5—N7	1.2496 (14)	N4—H4A	0.8600
O1—N6	1.2511 (15)	N4—H4B	0.8600
O6—N7	1.2577 (15)	N1—C1	1.3010 (17)
O4—N7	1.2476 (15)	N1—H1A	0.8600
O2—N6	1.2473 (15)	N1—H1B	0.8600
N5—C1	1.3477 (16)	N3—C2	1.3267 (16)
N5—C4	1.3767 (16)	N3—H3A	0.8600
N5—H5	0.8600	N3—H3B	0.8600
N2—C1	1.3531 (16)	C4—C3	1.3888 (17)
N2—C2	1.3822 (16)	C3—C2	1.3834 (18)
N2—H2	0.8600	C3—H3	0.9300
C1—N5—C4	122.26 (11)	H1A—N1—H1B	120.0
C1—N5—H5	118.9	C2—N3—H3A	120.0
C4—N5—H5	118.9	C2—N3—H3B	120.0
C1—N2—C2	122.27 (11)	H3A—N3—H3B	120.0
C1—N2—H2	118.9	N1—C1—N5	121.18 (12)
C2—N2—H2	118.9	N1—C1—N2	120.53 (12)
C4—N4—H4A	120.0	N5—C1—N2	118.28 (11)
C4—N4—H4B	120.0	N4—C4—N5	116.31 (11)
H4A—N4—H4B	120.0	N4—C4—C3	124.41 (12)
O2—N6—O1	120.68 (11)	N5—C4—C3	119.28 (11)
O2—N6—O3	118.54 (11)	C2—C3—C4	118.85 (12)
O1—N6—O3	120.78 (11)	C2—C3—H3	120.6
O4—N7—O5	119.59 (11)	C4—C3—H3	120.6
O4—N7—O6	120.46 (11)	N3—C2—N2	117.00 (11)
O5—N7—O6	119.94 (11)	N3—C2—C3	123.98 (12)
C1—N1—H1A	120.0	N2—C2—C3	119.02 (11)
C1—N1—H1B	120.0		
C4—N5—C1—N1	178.85 (11)	N4—C4—C3—C2	179.23 (12)
C4—N5—C1—N2	−0.76 (17)	N5—C4—C3—C2	−1.46 (17)
C2—N2—C1—N1	179.46 (11)	C1—N2—C2—N3	−178.59 (10)
C2—N2—C1—N5	−0.93 (17)	C1—N2—C2—C3	1.36 (17)
C1—N5—C4—N4	−178.68 (11)	C4—C3—C2—N3	179.81 (11)
C1—N5—C4—C3	1.96 (17)	C4—C3—C2—N2	−0.13 (17)

Hydrogen-bond geometry (Å, º)

D—H···*A*	*D*—H	H···*A*	*D*···*A*	*D*—H···*A*
N5—H5···O4	0.86	1.88	2.7321 (15)	174
N2—H2···O1^{i}	0.86	1.98	2.8319 (15)	169
N4—H4*A*···O6	0.86	2.08	2.9428 (15)	177
N4—H4*B*···O5^{ii}	0.86	2.43	3.0706 (16)	131
N4—H4*B*···O6^{ii}	0.86	2.11	2.9593 (15)	172
N4—H4*B*···N7^{ii}	0.86	2.62	3.4400 (16)	160
N1—H1*A*···O2	0.86	1.97	2.7986 (15)	160
N1—H1*A*···N6	0.86	2.69	3.3577 (16)	135
N1—H1*B*···O3^{i}	0.86	1.94	2.7912 (15)	172
N3—H3*A*···O3^{iii}	0.86	2.16	3.0018 (14)	167
N3—H3*A*···O2^{iii}	0.86	2.54	2.9770 (15)	113
N3—H3*B*···O5^{iii}	0.86	2.26	3.0619 (15)	156
C3—H3···O5^{iii}	0.93	2.56	3.3134 (16)	139

Symmetry codes: (i) −*x*+1, *y*−1/2, −*z*+3/2; (ii) −*x*+2, *y*−1/2, −*z*+1/2; (iii) *x*, *y*−1, *z*.